Pramāṇa – J. Phys., Vol. 28, No. 3, March 1987, pp. 257–267. © Printed in India.

Design studies of a 100 MeV proton linear accelerator

P SINGH, R MYTHILI and M G BETIGERI
Nuclear Physics Division, Bhabha Atomic Research Centre, Bombay 400 085, India

MS received 19 July 1986; revised 5 November 1986

Abstract. Design details of a 100 MeV proton linear accelerator (Alvarez system) operating at a resonating frequency of 400 MHz have been studied. Increase in the linac operating frequency has become feasible with the possibility of injecting protons from a radio frequency quadrupole accelerator with energies higher than the conventional pre-injectors. Various electrical parameters of such a system have been calculated and compared with the existing linac injectors operating at 200 MHz.

Keywords. Linac design calculation; radio frequency quadrupole-Alvarez combination; proton linear accelerator.

PACS No. 41·70

1. Introduction

In most of the proton linear accelerators operating in the world (Cole 1971; Wheeler *et al* 1979; Michaelis 1975) the configuration follows a familiar pattern in which protons from a d.c. source, usually a Cockcroft-Walton generator of 750 kV, are bunched and injected into an Alvarez type linear accelerator (linac) operating around 200 MHz. The choice of the exciting frequency of the Alvarez linear accelerator depends on the velocity of the proton beam (β) being injected into the linear accelerator. It has been shown (Smith 1959) that as long as the quantity $2\pi a/\beta\lambda \ll 1$, the longitudinal transit time factor is insensitive to the choice of the wavelength. For $2\pi a/\beta\lambda \gg 1$, the transit time factor falls exponentially and hence the effective shunt impedance of the structure drops rapidly. However, for $2\pi a/\beta\lambda = 1$, the transit time factor is 0·79 which is still a reasonable value for design purposes. Therefore, for a drift tube bore radius a of 1 cm and $\beta = 0{\cdot}04$ (corresponding to the 750 keV protons), the wavelength works out to 157 cm or a frequency of 191 MHz and hence the choice of 200 MHz for the exciting frequency in the existing linacs is not far from the calculated value.

However, on increasing the energy of the proton beam to be injected into the linac structure, two distinct advantages may be visualized. (i) Higher incident energy would allow injection of the proton beams into an Alvarez structure being operated at higher frequency. For $\beta = 0{\cdot}08$, which corresponds to a 3 MeV proton beam, the frequency for the Alvarez system would be 400 MHz. Higher operating frequency is expected to lead to lower rf losses. (ii) The injected protons are subjected to strong radial rf defocussing forces in the first stages of the linac cavity. The effect of these forces would be stronger for small velocities of the injected protons. Hence at a higher incident energy the requirements on the quadrupole magnets enclosed within the drift tubes are expected to be less stringent.

The prospect of providing intense, focussed and bunched beams at MeV energies is now being realized through the radio frequency quadrupole (RFQ) accelerator (Crandall *et al* 1979; Purser *et al* 1983). If the energy of the proton beam to be injected from such an accelerator is assumed to be 3 MeV, the practical transit time considerations suggest a minimum wavelength of 75 cm for the appropriate Alvarez system.

In order to study the details of such a system, a computer program LINAC was developed (§ 2) and was used to optimize the parameters for a 400 MHz Alvarez system (§3). The calculations have resulted in a physical design for a 100 MeV proton accelerator to be realized in four linac cavities of the Alvarez type. A comparison with existing linacs is attempted in § 4 to highlight the possible advantages of the present design.

2. Formalism

The calculation of the electromagnetic eigenvectors and eigenvalues in a linac cavity of the Alvarez type containing stemless drift tubes can be accomplished by solving finite difference approximations to the wave equation derived from Maxwell's equations. Assuming a cylindrical symmetry for the unit cell, the solutions of Maxwell's equations for the TM mode lead to the well-known Helmholtz equation for the magnetic field component (Katz 1970)

$$\frac{1}{r}\frac{\partial}{\partial r}\left[\frac{r\partial H_\varphi}{\partial r}\right]+\frac{\partial^2 H_\varphi}{\partial z^2}+\left[k^2-\frac{1}{r^2}\right]H_\varphi=0, \tag{1}$$

where k is related to the resonant frequency by

$$k=\omega(\varepsilon\mu)^{1/2}=2\pi f(\varepsilon\mu)^{1/2}=2\pi/\lambda. \tag{2}$$

Taking the quantity $F=rH_\varphi$ as a potential function the above equation simplifies to

$$\frac{\partial^2 F}{\partial r^2}+\frac{\partial^2 F}{\partial z^2}-\frac{1}{r}\frac{\partial F}{\partial r}+k^2F=0, \tag{3}$$

subject to the boundary condition $\partial F/\partial n=0$ on the conducting walls and symmetry planes and $F=0$ along the axis.

In view of the cylindrical symmetry and the periodic structure of the linac cavity along the z axis, the region of the meridian plane (z, r) in which this equation must be solved reduces to a quarter of a cell (figure 1).

Following standard methods (Austin *et al* 1965), the finite difference approach for a rectangularly bounded region (figure 1) is accomplished by superposing a finitely spaced square mesh upon the region such that the boundary of the region everywhere coincides with the mesh lines. For a typical mesh point (i, j) in the interior of the region, Taylor series expansions of the function F in terms of the potential function $F_{i,j}$ are

$$F_{i,j+1}=F_{i,j}+\frac{h\partial F_{i,j}}{\partial r}+\frac{h^2}{2}\frac{\partial^2 F_{i,j}}{\partial r^2}+O(h^3), \tag{4a}$$

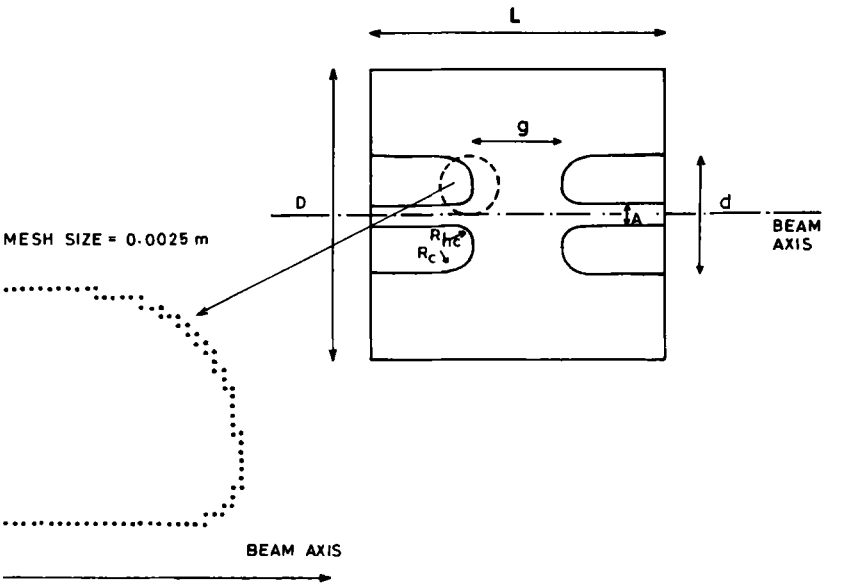

Figure 1. Unit cell geometry with cylindrical drift tube. Zigzag boundary used in the calculations is also shown.

$$F_{i,j-1} = F_{i,j} - \frac{h\partial F_{i,j}}{\partial r} + \frac{h^2}{2}\frac{\partial^2 F_{i,j}}{\partial r^2} - O(h^3), \tag{4b}$$

$$F_{i+1,j} = F_{i,j} + \frac{h\partial F_{i,j}}{\partial z} + \frac{h^2}{2}\frac{\partial^2 F_{i,j}}{\partial z^2} + O(h^3), \tag{4c}$$

$$F_{i-1,j} = F_{i,j} - \frac{h\partial F_{i,j}}{\partial z} + \frac{h^2}{2}\frac{\partial^2 F_{i,j}}{\partial z^2} - O(h^3), \tag{4d}$$

where h is the mesh spacing and $O(h^3)$ is the order of maximum error occurring due to the neglect of further terms in the expansion. Substitution of these equations into the scalar equation (3) yields

$$F_{i,j+1}\left(1 - \frac{h}{2r_j}\right) + F_{i,j-1}\left(1 + \frac{h}{2r_j}\right) + F_{i+1,j} + F_{i-1,j} + (k^2h^2 - 4)F_{i,j} + O(h^4) = 0. \tag{5}$$

The resultant error is of maximum order h^4. Therefore the smaller the mesh size, the smaller is the error. In the immediate vicinity of the boundary specifying the drift tube, the calculation of F values proceeds along a zigzag boundary made of mesh lines to approximate the smooth curvature (figure 1). The lowest eigenvalue for such a cavity is

given by

$$k^2 = -\frac{\sum_i \sum_j \left[\frac{F_{i,j}}{r_j}\left\{F_{i,j+1}\left(1-\frac{h}{2r_j}\right)+F_{i,j-1}\left(1+\frac{h}{2r_j}\right)+F_{i+1,j}+F_{i-1,j}-4F_{i,j}\right\}\right]}{\sum_i \sum_j \left[\left(\frac{F_{i,j}}{r_j}\right)^2\right]h^2}. \tag{6}$$

The formulation of the program follows the MESSYMESH code (MURA-713) closely.

The treatment of the cavity problem neglects the non-uniform spacing between the drift tubes and their unequal sizes. The resulting periodicity of the drift tube permits application of the boundary conditions along transverse planes at $z = 0, \pm L/2$ and the meridian plane ($0 \leqslant z \leqslant L/2, 0 \leqslant r \leqslant R$). An initial set of values for F are loaded onto the two-dimensional mesh such that one value of F is assigned to each point of intersection of a mesh line with another or with the boundary. Calculation of a trial eigenvalue is carried out. With this trial value for the eigenvalue the two-dimensional array of F values is improved. Repetitive calculations of F and k^2 proceeds until a stationary condition is reached such that the following convergence criteria are satisfied. (a) Eigenvalue convergence:

$$\left|\left[(k^{n+1}-k^n)/(k^{n+1})\right]\right| \leqslant 10^{-5}. \tag{7}$$

(b) Eigenvector convergence:

$$\left|\left[(F^{n+1}-F^n)/(F^{n+1})\right]\right| \leqslant 10^{-3}. \tag{8}$$

Once these criteria are satisfied, the potential values are used to calculate the auxiliary electromagnetic quantities (Katz 1970) namely the energy stored per unit volume, the power lost to the cavity walls per unit area, the quality factor, the average axial accelerating field, the shunt impedance, the transit time factor, the coupling coefficient and the peak surface electric field and its location.

3. Calculations

The calculations are done for a unit cell (figure 1). The geometry of the unit cell is specified by the parameters: D, the cavity diameter; L, the length of the unit cell ($\beta\lambda$); d, the drift tube diameter; R_c, the radius of curvature of the outer profile of the drift tube; R_{hc}, the radius of curvature of the drift tube bore hole corner and A, the diameter of the bore hole.

The code was checked by reproducing the MESSYMESH calculations reported in MURA-713. For the input parameters of MURA-713 (table 1) the auxiliary electromagnetic quantities were calculated. The calculations have been done for two unit cells namely linac cavity and laboratory cavity. The linac cavity consists of an outer wall of length L and two half-drift tubes (figure 2) while the laboratory cavity is of length $L/2$ with an end plate and a drift tube plate supporting a half-drift tube (figure 2). The lab cavity calculations are useful to optimize, in the initial stages, the performance of an actual cell to be adopted for fabrication. The results of the present calculations are compared with MURA-713 in table 1. Following the standard practice in all

Table 1. Linac cavity calculations (comparison with MURA-713 Run No. 30470).

Input parameters:	
Cavity diameter	= 88 cm
Drift tube diameter	= 16 cm
Diameter of the beam hole	= 3 cm
R_c	= 4 cm
R_{hc}	= 1 cm
g/L	= 0·34
Energy	= 51·36 MeV, β = 0·318
Frequency	= 202·82 MHz

Output parameters		Present calculation	Mura-713 Run No. 30470
1) Normalization factor to obtain 1 MV/m average axial electric field		598·70	562·01
2) Mesh size (mm)		2·50	5·00
3) Stored energy per unit volume (J/m^3)	W/V	1·689	1·600
4) Power dissipation (Watts)			
To cavity walls	PW1	4431·309	3829·46
To the end plate	PW2	2482·003	2283·04
To the drift tube plate	PW3	3497·109	3396·60
To the drift tube	PW4	3194·653	3353·98
5) Q-factor			
Linac cavity	Q_1	77684·70	79291·50
Lab cavity	Q_2	30250·00	30717·00
6) Shunt impedance MΩ/m			
Linac cavity	Z_1	61·630	65·340
Lab cavity	Z_2	23·990	25·310
7) Transit time factor		0·7951	0·7786
8) Coupling coefficient		0·0608	0·0652
9) Z_1T^2 (MΩ/m)		38·967	39·609
10) Z_1T^2/Q_1 (Ω/m)		501·61	499·54
11) Peak surface electric field E_p (MV/m)		5·436	4·901
12) Peak field location (cm)			
From the axis of drift tube		5·50	5·53
From end of drift tube		0·30	0·30
13) S (= E_2/E_1)		1·04	1·05

calculations, the average axial electric field is normalized to 1 MV/m and the resulting scaling factors for the different cavities utilized to obtain the stored energy per unit volume and the power losses. The quantities Q_1, Z_1 correspond to the linac cavity while the quantities Q_2, Z_2 correspond to the lab cavity.

One of the criteria to test the consistency of the potential values is to compare the average electric field along the axis computed in two ways

$$E_1 = \frac{1}{\omega\varepsilon L}\int_0^L \frac{1}{r}\left|\frac{\partial F}{\partial r}\right|_{r=0} \mathrm{d}z \tag{9a}$$

and

$$E_2 = \frac{\omega\mu}{L}\int_0^R\int_0^L \frac{F}{r}\,\mathrm{d}r\,\mathrm{d}z. \tag{9b}$$

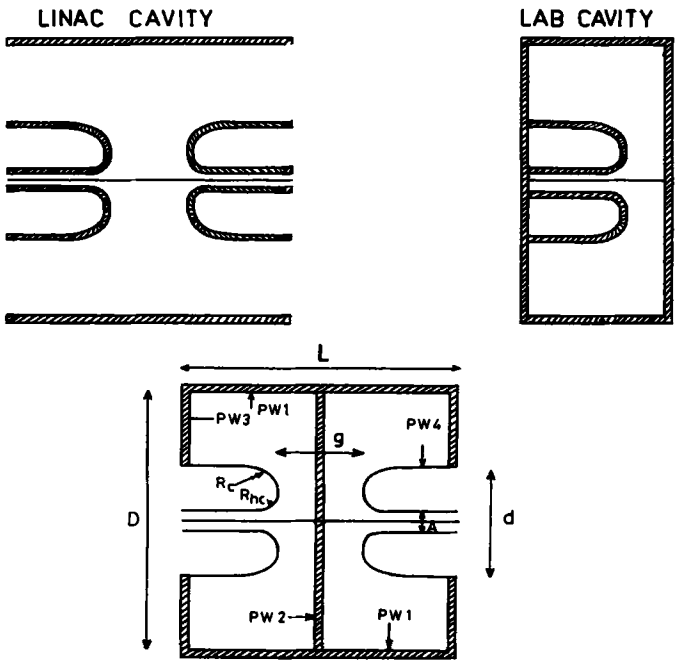

Figure 2. Linac and lab cavity-unit cell.

Their ratio $S = E_2/E_1$ is a good measurement of the consistency of the solution. Typically in the present calculations, S is of the order of 1·04 as compared with 1·05 for the MESSYMESH code, 1·02 in IDDA (Katz 1968) and 1·005 in CLAS (Martini and Warner 1968).

A further check on the program "LINAC" consisted in satisfactory reproduction of the auxiliary electromagnetic quantities for the input parameters at various energies as reported for the BNL 200 MeV linac (Wheeler *et al* 1979). After being satisfied with the program, the calculations for the unit cells at various energies for an Alvarez type cavity operating at 400 MHz were done. The diameter for a hollow cylindrical cavity excited in the lowest TM_{010} mode is given by

$$D = (2 * 2{\cdot}405)/k, \tag{10}$$

which works out to 57·42 cm for an operating frequency of 400 MHz.

However, we found that the inclusion of the drift tubes decreases the resonating frequency. Therefore to resonate the cavity at the same frequency the diameter of the cavity was reduced. In our calculations we have chosen D = 46–42 cm. The bore radius a was fixed at 1 cm for tanks at the low β end of the linac from the transit time considerations and was kept the same for all the other tanks. In view of the need to provide quadrupoles inside the drift tubes, the drift tube diameter was fixed to 12 cm. A value of 1 cm for R_{hc} was fixed for all the tanks. Choice of the other geometrical parameters g/L and R_c was made consistent with the desired resonant frequency. Variation of the frequency as a function of g/L for different values of D and d is shown in figure 3 for a proton energy of 55 MeV. Once the geometrical parameters were

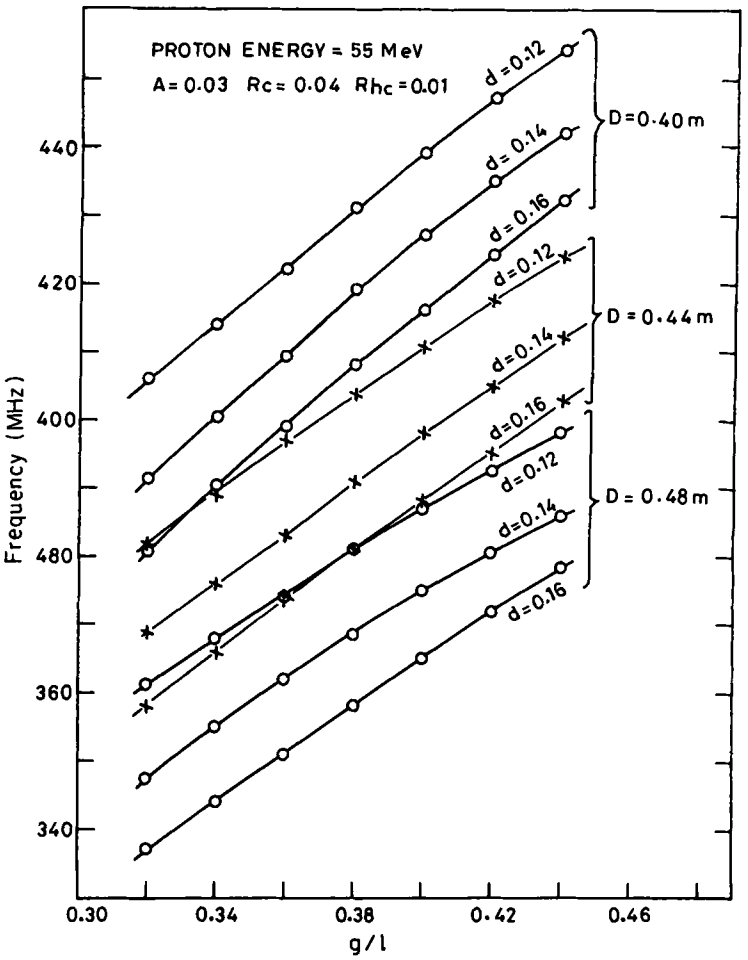

Figure 3. Variation of resonating frequency with g/L for different values of cavity and drift tube diameters.

decided, a mesh spacing was introduced in the meridian plane (z, r) and the eigenvector $F(z, r)$ was defined at the nodal points as

$$F(z, r) = F(ih, jh) = F_{i,j} \tag{11}$$

for integer values of i and j. An initial trial eigenvector was assigned. Eigenvector $F_{i,j}$ distribution was calculated in the desired region using an over relaxation successive displacement iterative procedure (Klemperer and Barnett 1971). Iterations were continued till the convergence criteria mentioned earlier were satisfied and the final set of potential values used to calculate various electrical parameters (table 2).

For the purpose of the present calculations, it was assumed that the protons gain a total energy of 100 MeV in four stages: 7 MeV in the first tank and 30 MeV each in the subsequent three tanks.

Table 2. Parameters for 400 MHz Alvarez linac cavities.

Diameter of beam hole = 0·02 m	Average axial electric field = 1·0 MV/m										
Drift tube diameter = 0·12 m	Mesh size = 0·001 m (3 MeV); 0·0025 m (all others)										
Proton energy (MeV)	3	6·5	10	10	25	40	55	70	70	85	100
Cavity diameter (m)	0·46	0·46	0·46	0·44	0·44	0·44	0·44	0·44	0·42	0·42	0·42
R_c (m)	0·02	0·03	0·03	0·04	0·04	0·04	0·04	0·04	0·04	0·04	0·04
g/L	0·2	0·26	0·305	0·22	0·31	0·345	0·375	0·41	0·37	0·39	0·405
Q_1 (10^4)	4·96	5·36	5·35	5·02	5·21	5·25	5·21	5·15	4·68	4·62	4·56
Z_1 (MΩ/m)	60·3	73·1	70·8	69·9	71·7	72·5	71·3	70·2	61·9	60·6	59·1
T	0·65	0·73	0·78	0·81	0·81	0·77	0·74	0·71	0·76	0·73	0·71
C^*	0·09	0·08	0·06	0·05	0·06	0·07	0·08	0·09	0·07	0·08	0·08
Energy stored (J/m^3)	2·08	1·95	2·04	2·08	2·08	2·04	2·05	2·06	2·33	2·34	2·4
Peak surface electric field (MV/m)	3·87	5·37	5·29	6·98	5·73	5·31	5·2	5·2	5·58	5·5	5·58

* Coupling coefficient

Table 3. Kilpatrick's limit.

Frequency (MHz)	Peak surface field (MV/m)
7·5	5
70·0	10
209·4	15
378·5	19
428·8	20

In the present program, the maximum field E_p on the surface of a drift tube for an average axial electric field of 1 MV/m has been calculated. The maximum safe limit to the value of peak surface electric field has been given by Kilpatrick (1953) in the relationship

$$f = 1{\cdot}64\, E_{SL}^2 \exp[-8{\cdot}5/E_{SL}] \tag{12}$$

where f is the frequency in MHz and E_{SL} is the value of surface electric field in MV/m above which sparking is possible. For different values of E_{SL}, f has been calculated and are listed in table 3. For Alvarez structures operating at 400 MHz, the sparking limit allows the peak surface field value E_{SL} to be 19·5 MV/m. One may therefore scale up the average axial electric field E_0 by a ratio E_{max}/E_p where E_{max} is the maximum permitted electric field ($E_{max} < E_{SL}$) used in the calculations. The parameters for the 100 MeV linac have been worked out and are listed in table 4. The rf power P per energy gain ΔW, is given by

$$P/\Delta W = E_0 T/ZT^2 \cos\phi \tag{13}$$

The power has to be increased over a value computed from the theoretical value of Z, the shunt impedance, to allow for losses on drift tube stems, tuners, end plates, rf contacts, spring rings, pump out ports, surface roughness and contamination. The

Table 4. Typical parameters for a 100 mA-100 MeV linac.

Frequency = 400 MHz $\cos\varphi = 0{\cdot}90$	Total power = 19·01 MW Total cavity length = 42·5 m			
Cavity number	1	2	3	4
Input energy (MeV)	3	10	40	70
Output energy (MeV)	10	40	70	100
Energy gain (ΔW)	7	30	30	30
D (cm)	46	44	44	42
d (cm)	12	12	12	12
A^1 (cm)	2	2	2	2
R_c (cm)	2	4	4	4
R_{hc} (cm)	1	1	1	1
g/L (range)	0·20–0·305	0·22–0·345	0·345–0·41	0·37–0·405
E_0 (MV/m)	3·0	3·17	3·63	3·42
E_g (MV/m)	18·7–9·0	12·3–10·4	10·4–8·9	9·2–8·4
E_{max} (MV/m) (surface)	14·5	19	19	19
$\langle T \rangle$	0·72	0·80	0·74	0·73
$\Delta W/\Sigma L$	1·94	2·28	2·42	2·25
Cavity length (m)	3·6	13·1	12·4	13·4
$\langle ZT^2 \rangle$ (MΩ/m)	35·77	45·43	39·01	32·63
Power (practical) (MW)	0·61	2·42	2·98	3·31
κ	1·3	1·3	1·3	1·3
RF power (practical) (MW) (including beam power)	1·31	5·42	5·98	6·31

[1] A is the beam hole diameter i.e. $A = 2a$

power will thus be increased by a factor κ and in the present design a value of $\kappa = 1{\cdot}3$ has been assumed. The radio frequency power for beam loading also has to be provided. The total rf power listed in table 4 includes the beam power for a 100 mA proton beam.

4. Discussion

A large number of parameter variations, with the cavity resonating at 400 MHz were tried out and the values in table 2 are the culmination of these calculations. An increase in D produces large Z; however, it results in smaller T. Similarly a decrease in the value of d improves the value of ZT^2 slightly. The present calculations assume $d = 12$ cm and $a = 1$ cm. Further reduction in these parameters may improve ZT^2 but would lead to an impractical design. The use of higher frequency for the linac system results in a high value of E_{SL} and hence a high value for E_0 which in turn leads to a smaller length for the accelerator. However the radio frequency power lost on the cavity walls scales as α^2 where $\alpha = E_{max}/E_p$. A comparison of the present parameters with the BNL linac (Wheeler *et al* 1979) is listed in table 5. It may be noted that the reduction in the transit time factor in the present calculations amounts to less than 5 % as compared to the BNL accelerator. The parameters of linac injector to the spallation neutron source (Boardman 1982) are compared with our calculations in table 6. In spite of the higher frequency, the values of ZT^2 achieved in the present calculations are comparable with the ones obtained in the BNL machine. The usual statement that the higher the

Table 5. Comparison of the present calculations with BNL data.

	Present calculations				BNL data			
	1	2	3	4	1	2	3	4
Proton energy (MeV)	3–10	10–40	40–70	70–100	0·75–10·42	10·42–37·54	37·54–66·18	66·18–92·55
Energy gain (MeV)	7	30	30	30	9·67	27·12	28·64	26·37
Cavity length (m)	3·61	13·16	12·4	13·33	7·44	19·02	16·53	16·68
Cavity diameter (m)	0·46	0·44	0·44	0·42	0·94	0·9	0·88	0·88
Drift tube diameter (m)	0·12	0·12	0·12	0·12	0·18	0·16	0·16	0·16
Bore hole diameter (m)	0·02	0·02	0·02	0·02	0·02–0·025	0·03	0·03	0·03
R_c (m)	0·02–0·03	0·04	0·04	0·04	0·02	0·04	0·04	0·04
R_{hc} (m)	0·01	0·01	0·01	0·01	0·005	0·01	0·01	0·01
g/L	0·2–0·305	0·22–0·34	0·345–0·41	0·37–0·405	0·21–0·31	0·2–0·31	0·3–0·36	0·37–0·41
T	0·65–0·78	0·81–0·77	0·77–0·71	0·76–0·71	0·64–0·81	0·86–0·81	0·82–0·75	0·75–0·69
ZT^2 (MΩ/m)	25·5–42·9	46–42·8	42·8–35·5	35·5–29·8	27–47·9	53·5–44·8	44·6–35·2	35–28·5
Average axial field (MV/m)	3·0	3·17	3·63	3·42	1·6–2·31	2·0	2·6	2·6
Cavity excitation power (practical) (MW)	0·61	2·42	2·98	3·31	0·51	1·4	2·36	2·57
κ factor	1·3	1·3	1·3	1·3	1·3	1·35	1·35	1·4
Total power (practical) (MW) for 100 mA	1·31	5·42	5·98	6·31	1·48	4·12	5·22	5·21

Table 6. Comparison of the present calculations with the SNS injector data.

Parameters	Present calculations			SNS data			
cavity #	1	2	3	1	2	3	4
Output energy (MeV)	10	40	70	9·92	30·47	49·76	70·5
Length (m)	3·6	13·1	12·4	7·15	11·96	11·24	12·11
Accelerating rate (MV/m)	3·0	3·17	3·63	0·8–1·5	1·72	1·71	1·7–1·6
Power-theory (MW)	0·47	1·86	2·29	0·44	1·31	1·4	1·5
κ-factor	1·30	1·30	1·30	1·24	1·20	1·43	1·20
Total power (practical) for 20 mA (MW)	0·75	3·02	3·58	0·73	1·99	2·39	2·22

frequency at which the Alvarez is operated, the lower are the power losses (Wheeler *et al* 1979) must therefore be treated with caution. However, the resulting reduction in the sizes (both the diameter and the length) as compared to the 200 MHz structure is expected to lead to a substantial reduction in costs.

References

Austin B, Edwards T W, O'Meara J E, Palmer M L, Swenson D A and Young D E 1965 Report MURA-713

Boardman B (Ed.) 1982 Rutherford Appelton Laboratory Report RL-82-006

Cole F T 1971 *Particle Accelerators* **2** 1

Crandall K R, Stokes R H and Wangler T P 1979 *Proc. 10th Linear Accelerator Conf. Montauk*, New York Sept. 9–14, Brookhaven National Laboratory 1980 Report BNL-51134 p. 205

Katz A 1968 Saclay thesis (Unpublished)

Katz A 1970 *Linear accelerator* (eds) P M Lapostolle and A L Septier (Amsterdam: N. H. Publishing Company)

Kilpatrick W D 1953 A criterion for vacuum sparking design to include both R. F and D. C, Radiation Lab Report UCRL-2321

Klemperer O and Barnett M E 1971 *Electron optics* (Cambridge: University Press) III ed.

Martini M and Warner D J 1968 CERN- Report 68-11

Michaelis E 1975 *Proc. Particle Accelerator Conf., Washington, USA* 1975 *IEEE NS Trans.* **22** 1385

Purser F O, Wadlinger E A, Sander O R, Potter J M and Crandall K R 1983 *IEEE NS* **30** 3582

Smith Lloyd 1959 *Encyclopedia of physics* (ed.) S Flugge **44** 341

Wheeler G W, Batchelor K, Chasman R, Grand P and Sheeman J 1979 *Particle Accelerators* **9** 1